Enhanced Accuracy for a Complex Image Theory Position Estimator using Frequency Diversity

Matthew S. Trotter #, Joshua D. Griffin #, and David S. Ricketts *

#Disney Research, Pittsburgh, PA, 15219, USA.
*North Carolina State University, Raleigh, NC, 27695, USA.

***Abstract*— Complex image theory has been proposed as a means to efficiently calculate the fields induced by a magnetoquasistatic source above the earth. In position location applications, this has enabled an accurate determination of position from measured field strengths. While promising, complex image theory is only an approximation of the true field; inherent errors in position estimation occur due to the limitations of this approximation. In this work we show that the estimation errors are frequency dependent and that by combining multiple frequency signals, the overall RMS estimation error can be significantly reduced. We demonstrate this by finding the estimation error over an x-y plane of 20 m for two frequencies individually and then combined. Our results show a 12.9 % and 45.2 % reduction in position error over the respective individual frequencies.**

***Index Terms*— complex image theory, frequency diversity, quasistatic, magnetoquasistatic.**

I. Introduction

Position tracking using magnetoquasistatic fields is an attractive method for applications where line-of-sight signals are not viable or in the presence of weakly conducting obstructions, such as the human body. In applicaitons where the position location is desired above the earth, the image fields generated by the earth need to be accounted for to obtain an accurate position. In [1], a magnetoquasistatic positioning system was proposed that used complex image theory (CIT) to account for the effects of the image fields in the earth as it is computationally more efficient than the exact integral equations for the electric and magnetic fields [2]-[3]. Previous studies have shown that position estimation errors arise due to the approximation made by CIT [1], and thus potentially limit the accuracy of position estimation using CIT.

In this work, we show that the estimation error of CIT is position and frequency dependent, with error varying at a fixed location as frequency is changed and the error varying at a fixed frequency as the distance is changed. By leveraging the variation of error with frequency, we show that a multi-frequency positioning system can combine the fields to obtain a lower overal estimation error than a single-frequency system. This paper shows simulated reduction of position-estimation errors over a two-dimensional space by averaging the position estimations from two different frequencies. The averaged results show a 12.9% and 45.2% reduction of the RMS error across the two-dimensional space when compared to the two single-frequency cases.

II. Frequency Dependence of the CIT Approximation

The exact integral equation for magnetic flux density $\vec{B}$ in the quasistatic region of a transmitting loop antenna can be split into two components: First, there is the contribution from the transmitting loop itself and second the contribution from eddy currents induced in the ground plane [3]. From the geometry of Fig. 1, the flux density contribution from the transmitting loop is characterized by the flux density from a simple magnetic dipole [4]:

$$\begin{aligned}&\vec{B}(\vec{R}_0,\vec{m}_\mathrm{s}) = \\ &\left(\frac{-k^3\mu_o}{4\pi}\right)\left\{\left[\frac{1}{(kR_0)^3}+\frac{j}{(kR_0)^2}\right](1-3\hat{R}_0\hat{R}_0\,\cdot)\vec{m}_\mathrm{s}\right. \\ &\left.+\left(\frac{1}{kR_0}\right)\hat{R}_0\times(\hat{R}_0\times\vec{m}_\mathrm{s})\right\}e^{-jkR_0},\end{aligned} \tag{1}$$

This approximation is very accurate at distances beyond ten times the transmitting loop radius [5]. In this work, the simulated loop radius is 8 cm, thus, the approximation of the fields from the transmitting loop alone is accurate for distances $R_0 > 80$ cm. The eddy currents induced in the ground plane are approximated in CIT very simply by an image of the transmitting magnetic dipole located at a complex-valued depth $h + \delta(1 - j)$ below the surface. Here, $\delta = \sqrt{2/(\omega\mu_2\sigma_2)}$ is the skin depth. The flux density contribution from the image uses (1) with the complex-valued position vector $\vec{R}_2$ and magnetic moment $\vec{m}_\mathrm{im}$ substituted in place of $\vec{R}_0$ and $\vec{m}_\mathrm{s}$, respectively.

The image dipole is the main source of error in the CIT approximation and exhibits frequency dependence. As an illustrative example, Fig. 2 shows the estimation error up to a distance of 22 m for frequencies spaced by a factor of $\sqrt{2}$. The estimator uses CIT to get the x-coordinate of the position assuming y, z, and orientation are known a-priori. The input to the estimator is the magnetic flux density produced by the exact integral formulation. No noise was introduced; therefore, the only source of error is

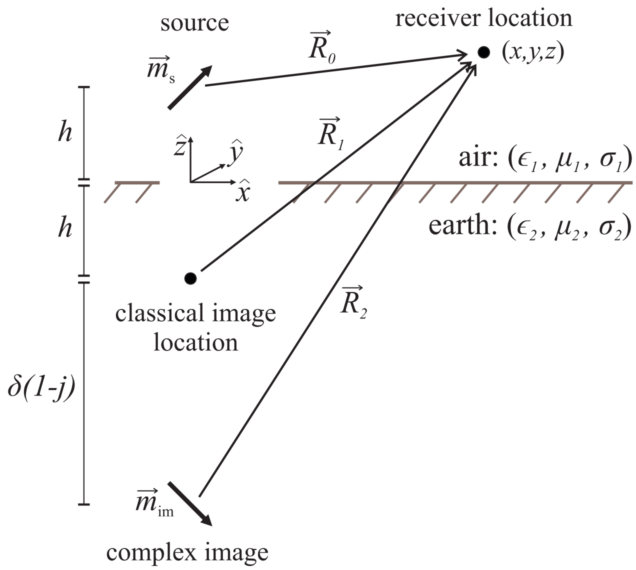

Fig. 1. Geometry for a transmitting loop of current above a semi-infinite earth.

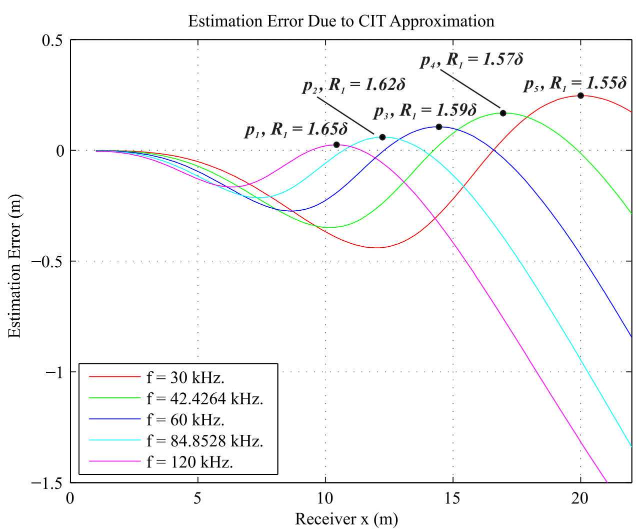

Fig. 2. The location of maximum estimation error for each frequency due to the CIT approximation occurs at approximately $R_1 = 1.6\delta$.

the differences in flux density predicted by CIT over the exact integral.

Fig. 2 shows that the error curve shifts to the left as frequency increases and the initial oscillatory portion reduces in magnitude; note that the error at larger distances increases with increased frequency. Thus, as frequency increases, the error at short distances becomes smaller, but the error at longer distances becomes larger. Horizontally, the error curve moves left and reduces in amplitude at short distances by approximately by a factor of two when the frequency is quadrupled. This observation is explained in detail by [6] where it was found that the locations of highest approximation error occur at approximately the same R_1-distance expressed in skin depths. For example, Fig. 2 shows that the locations of maximum estimation error $(p_1, \ldots, p_5)$ are located at $R_1 \approx 1.6\delta$ with a small offset depending on the frequency. Thus, the error curves compress horizontally approximately proportional to $1/\sqrt{f}$ since $\delta \propto 1/\sqrt{f}$.

The estimation error can be improved by using the higher-frequency fields at short distances and the lower-frequency fields at longer distances. Since we do not know where our location is, a simple algorithm is needed. We propose the averaging of the the multi-frequncy fields to reduce the errors accross all locations. According to the graph shown, frequencies that are separated by a factor of two provide the best complementing error curves. The frequencies of 30 kHz and 60 kHz are chosen for the two-dimensional simulation in the next section. It will be seen that the benefits of error reduction in the one-dimensional case extend to the two dimensional case as well.

III. Two-Dimensional Reduction of Estimation Errors

To illustrate our proposed error reduction technique using multiple frequencies, we simulated the x-coordinate estimation errors in a two-dimensional space above a semi-infinite ground plane at 30 kHz and 60 kHz. A transmitting loop antenna is located in air $(\epsilon_0, \mu_0, 0\ \mathrm{S/m})$ 1 m above the earth $(\epsilon_0, \mu_0, 0.05\ \mathrm{S/m})$ at the location (0, 0, 1) m and is oriented such that its magnetic dipole moment is pointed in the z-direction. The receiver measures the z-component of the magnetic flux density B_z in the x-y plane located 1.5 m above the earth. The measurement is simulated by numerically evaluating the exact integral formula for the magnetic flux density B_z. Then, this measured value of B_z is input into the CIT estimator, which produces an estimation for the x-coordinate by inverting the CIT algebraic equations. The position coordinates y and z and also the orientation of the transmitter is known to the estimator a-priori. The estimation error is the difference $\hat{x} - x$ between the estimated value $\hat{x}$ and the true value x. Positive error means the estimator is producing values ”too far” while negative values are ”too close”.

Fig. 3 shows the frequency dependence of estimation errors of x using the frequencies 30 kHz and 60 kHz individually. For the 30 kHz case, the large band of positive error (in red and red-orange) is located approximately between 18.5 m and 23 m from the origin of the plot. And this same large band of positive error is located between 12.75 m and 16.75 m from the origin of the plot for the 60 kHz case. In terms of skin depths, these bands are both located between approximately 1.4δ and 1.8δ. These bands are offset from one another, which allows averaging to work.

Fig. 4 shows that the overall estimation error reduced by averaging the two single-frequency estimations, (i.e.

(a)

(b)

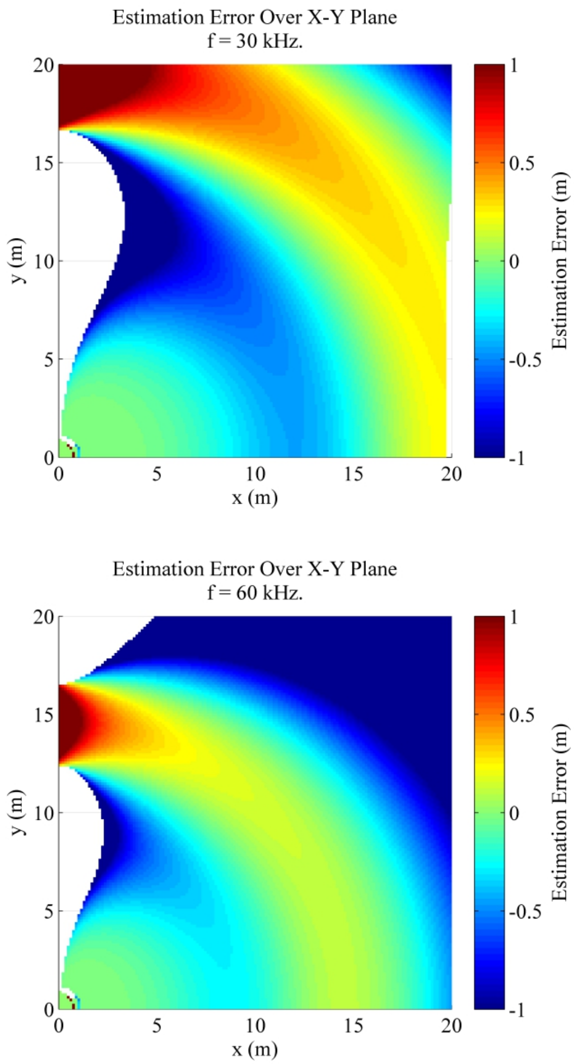

Fig. 3. Estimation error $\hat{x} - x$ across the x-y plane where $z = 1.5$ m for a system frequency of (a) 30 kHz and (b) 60 kHz individually. Blank areas represent estimations outside the bounds $x \in (0, 20)$ m.

$\hat{x} = (\hat{x}_{30} + \hat{x}_{60})/2$). The RMS error across the entire two-dimensional plane plotted for the combined case is 48.1 cm. On the other hand, the RMS error is 55.2 cm for the 30 kHz case and 87.8 cm for the 60 kHz case, which is a reduction of 12.9% and 45.2% respectively.

The technique may be applied to three dimensions. Further improvements such as weightings and multiple frequencies can improve on the results of this simulation.

IV. Conclusion

We presented an analysis of CIT position estimation error versus frequency and showed that the frequency dependence of the error can be used to reduce overall estimation error. An averaging technique was demonstrated that combined position estimations from independent simulations of a 30 kHz system and a 60 kHz system. The estimation error using both frequencies showed a reduction of the RMS error of 12.9% from the 30 kHz case and 45.2% from the 60 kHz case over the two-dimensional x-y plane simulated. More intelligent or complex combining techniques can be studied to further reduce the estimation error.

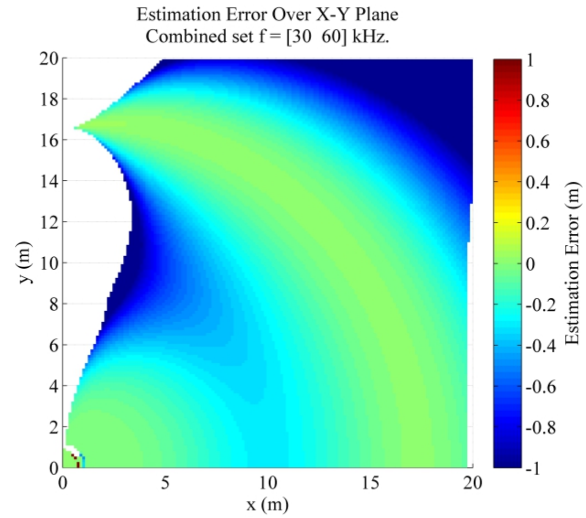

Fig. 4. Estimation error $\hat{x} - x$ using simple averaging of the estimations using 30 kHz and 60 kHz across the same x-y plane. Blank areas represent estimations outside the bounds $x \in (0, 20)$ m.

References

[1] D. D. Arumugam, J. D. Griffin, and D. D. Stancil, "Experimental demonstration of complex image theory and application to position measurement," *IEEE Antennas and Wireless Propagation Letters*, vol. 10, pp. 282 –285, 2011.

[2] J. R. Wait and K. P. Spies, "On the image representation of the quasi-static fields of a line current source above the ground." *Canadian Journal of Physics*, vol. 47, pp. 2731–2733, 1969.

[3] J. T. Weaver, "Image theory for an arbitrary quasi-static field in the presence of a conducting half space," *Radio Science*, vol. 6, pp. 647–653, 1971.

[4] G. S. Smith, *An Introduction to Classical Electromagnetic Radiation*. Cambridge University Press, 1997.

[5] D. Arumugam, J. Griffin, D. Stancil, and D. Ricketts, "Higher order loop corrections for short range magnetoquasistatic position tracking," in *Antennas and Propagation (APSURSI), 2011 IEEE International Symposium on*, 2011, pp. 1755–1757.

[6] P. R. Bannister, "Applications of complex image theory," *Radio Science*, vol. 21, pp. 605–616, 1986.